

# We are IntechOpen, the world's leading publisher of Open Access books Built by scientists, for scientists

6,900

Open access books available

186,000

International authors and editors

200M

Downloads

Our authors are among the

154

Countries delivered to

TOP 1%

most cited scientists

12.2%

Contributors from top 500 universities



WEB OF SCIENCE™

Selection of our books indexed in the Book Citation Index  
in Web of Science™ Core Collection (BKCI)

Interested in publishing with us?  
Contact [book.department@intechopen.com](mailto:book.department@intechopen.com)

Numbers displayed above are based on latest data collected.  
For more information visit [www.intechopen.com](http://www.intechopen.com)



---

# Composite Blades of Wind Turbine: Design, Stress Analysis, Aeroelasticity, and Fatigue

---

Ahmad Reza Ghasemi and Masood Mohandes

Additional information is available at the end of the chapter

<http://dx.doi.org/10.5772/63446>

---

## Abstract

In this chapter, four main topics in composite blades of wind turbines including design, stress analysis, aeroelasticity, and fatigue are studied. For static analysis, finite element method (FEM) is applied and the critical zone is extracted. Moreover, geometry, layup, and loading of the turbine blades made of laminated composites are calculated and evaluated. Then, according to the stress analysis, critical layer is specified and safety factor is studied based on Tsai-Wu failure criterion. Aeroelasticity is the main source of instability in structures that are subjected to aerodynamic forces. One of the major reasons of instability is the coupling of bending and torsional vibration of flexible bodies, which is known as flutter and considered in this study. Numerical and analytical methods are applied for considering the flutter phenomenon of the blades. For numerical method, the FEM and Joint Aviation Requirements (JAR-23) standard and for analytical method, two-degree freedom flutter and Lagrange's equations are utilized. Also, lifetime prediction of a horizontal axis wind turbine composite blade is investigated. Accumulated fatigue damage modeling is employed as a damage estimation rule based on generalized material property degradation.

**Keywords:** wind turbine, composite blade, aeroelasticity, fatigue, finite element method

---

## 1. Introduction

### 1.1. Wind turbine

Using wind turbine as electricity generator has some advantages and disadvantages. Some advantages of using wind turbines for electricity generation are electricity generation without

---

any pollution, fast installation and commissioning, and also low expense for maintenance. Although electricity generation by the wind turbine has some advantages, it has some disadvantages, too that its main disadvantage is the temporary nature of wind flow. Therefore, utilizing efficient equipment is necessary in order to get as much as energy from wind during the limited period of time that it flows strongly.

## 1.2. Composite blades

One of the most important components of a wind turbine is blade. A beam model of a wind turbine blade is generally suitable for structural-dynamic analysis. It will differ from the small-deflection theory beam models used in conventional analyses of non-rotating structures, and it is more like the beam-column representations used in elastic stability analysis. Four main topics in blade of the wind turbines that should be considered are designing, stress analysis, aeroelasticity, and fatigue.

## 1.3. Literature review

Development and application of wind turbines and the related issues such as structural design, aerodynamic design, and material selection as well as manufacturing issues, including fatigue, optimization, and aeroelastic stability have attracted researchers' attention. Jureczko et al. [1] presented a model for the design and optimization of wind turbine blades and development an ANSYS program that implements a modified genetic algorithm enables optimization of various objective functions subjective to various constraints such as thicknesses and main dimensions of the model blade. Guo [2] studied weight optimization and aeroelasticity of aircraft wing structure analytically and numerically and compared the results with experimental results. Veers et al. [3] considered the design, manufacture, and evaluation of wind turbine blades. They also verified and improved blade design with detailed stress analysis. Baumgart [4] presented a mathematical model for an elastic wind turbine blade and compared analytical and experimental results. Nonlinear rotor dynamic stimulation of wind turbine by parametric excitation of both linear and nonlinear terms caused by centrifugal and Coriolis forces was investigated by Larsen and Nielsen [5].

The fundamental aspects and the major issues related to the design of offshore wind turbines were outlined by Petrini et al. [6]. They considered the decomposition of these structural systems, the required performance, and the acting loads. Lee et al. [7] numerically investigated the load reduction of large wind turbine blades using active aerodynamic load control devices, namely trailing edge flaps. Tenguria et al. [8] studied the design and analysis of large horizontal axis wind turbine, and NACA airfoils were taken for the blade from root to tip.

Every structure under the influence of aerodynamic forces has specific performance that can change its properties and structure constants such as stiffness coefficient and natural frequencies. Therefore, the structure is faced with strong instabilities that cannot be prevented even by increasing the reliability of the design. This destruction has been created due to a specific force, and this value of force is created because of a specific relative velocity of flow that is called flutter phenomenon, and the fluid speed destruction is called flutter speed [9]. Recog-

nizing the flutter speed, we can ensure the safety of structure under aerodynamic forces. In structures such as a plane, flutter speed is considered as the limiting velocity. Limiting velocity is the velocity which must not be reached by an aircraft under any circumstances.

To ensure the safety of aerospace structures against aeroelastic instability, the Joint Aviation Requirements (JAR) [10] standard is used. Based on JAR-23, preventing flutter in the vicinity of fluid velocity can be ensured, if natural frequencies of the bending and torsion are isolated. Shokrieh and Taheri [11] conducted a numerical and experimental study of aeroelastic stability of composite blades of aircrafts based on this standard. Baxevanou et al. [12] described a new aeroelastic numerical model, which combines a Navier-Stokes CFD solver with an elastic model and two coupling schemes for the study of the aeroelastic behavior of wind turbine blades undergoing classical flutter. Fazelzadeh et al. [13] studied the coupling of bending-torsional flutter of a wing containing an arbitrarily placed mass under a driving force. Results are indicative of the important influence of the location and magnitude of the mass and the driving force on the flutter speed and the frequency of the aircraft wing. Lee et al. [14] investigated the performance and aeroelastic characteristics of wind turbine blades based on flexible multibody dynamics, a new aerodynamic model, and the fluid-structure interaction approach. They proposed a new aerodynamic model based on modified strip theory (MST).

Some researches have been done on the fatigue phenomenon of the blades. In the most of them, in the first step, load spectra obtained by digital sampling of strain gauges which read the strain at a specific location near the root of blade has been used. In the second one, the weight of each load spectrum is obtained by its rate of occurrence. Finally, total load spectrum, which is obtained by the summation of all weighted load spectra, is used to estimate fatigue damage in the blade using Miner's rule [15]. This rule has some defects that linear nature is its main weakness. Investigations have shown that Miner's rule is not proper for fatigue consideration in both metals and composites [16]. Also, another shortcoming of this rule lies in simulation of the load sequence and history of load events which is seen in the difference of predicted lifetimes of blades with two orders of magnitudes for two load cases with different load sequences [15]. Admittedly many researches have considered the fatigue simulation of the composite blades, but the most of them have focused on the deterministic approach. Furthermore, there are other problems for fatigue in the blades by these methods such as recognizing a place to install the strain gauges in order to extract the load spectrum and also using a massive and high-cost material fatigue database.

The main reason to create fatigue in the wind turbine blades is cyclic loads. Variation of wind speed, annual gust, rotation of rotor, and variation of weight vector direction toward the local position of the blade [17] are the production sources of the cyclic loads. These sources have different effects on the cyclic load. The two first sources change the total amount of the load. Also, rotation of rotor produces fluctuating load with a frequency identical to the rotor rotation frequency. Last one is the effect of wind shear which arises from change of wind speed by changing in height.

Considering the effect of wind shear in the design process is not necessary, because its influence on the fatigue damage is negligible [18]. Moreover, gust phenomenon is studied annually based on the Germanischer Lloyd's standard [19]. During gust occurrence, vibration is created

in the blade due to the gust impact effect, which arises the linear combination of its mode shapes. Eggleston and Stoddard [20] investigated engineering design of wind turbine. The results of their study showed that the first mode shape had the most significant role in displacements. Furthermore, the effect of wind direction on the turbine blades is not considerable, because the turbine always stays upwind and with changing the wind direction, the active yaw control system will adapt the turbine with new direction of wind vector as quickly as possible. Therefore, after defining cyclic loading sources, all corresponding applied stresses are derived from full range static analyses covering all events [17].

Designing, stress analysis, aeroelasticity, and fatigue of a composite blade wind turbine are investigated in this chapter. First, the geometry of blades is designed using the finite element method (FEM) for considered materials and layups. Then, using the static and dynamic analyses of the blades, the critical zone and flutter phenomenon are considered. Also, the damage is estimated utilizing accumulated fatigue damage modeling.

## 2. Problem description

Designing of the blades to get the maximum energy from the wind flow is an essential topic which is according to a refined aerodynamic science. Stiffness and strength to weight ratios are two important parameters to design the blades. Blades of horizontal axis are now completely made of composite materials that not only have they lower weight and appropriate stiffness, but also providing good resistance to the static, dynamic, and fatigue loadings. To attain the highest possible power output from the wind turbine under specified atmospheric conditions, changing two parameters are necessary. The first is change of the dynamic and mechanical properties of the wind turbine blade which modify the composite material, which the blade is made of it, and the second is changing shape of the blade. Admittedly change of the shape of blade modifies the stiffness and stability, but it may influence aerodynamic efficiency of wind turbine. Therefore, specifying the optimal shape of blade and optimal composite material are an important and complex problem. Nevertheless, selection of airfoil and also calculating the loading are two significant topics to design the composite blade.

## 3. Design of the blade

### 3.1. Finite element modeling

For finite element (FE), analysis of the turbine blade, the ANSYS commercial software is used. The FEM is provided according to dimensions of 660 kW composite wind turbine blades, and an airfoil is selected appropriately, as well as most popular design methods [14, 21]. Geometric dimensions of the blade structure are shown in **Table 1**. To carry aerodynamic forces, the weight of the blade, bending moment in blade and other forces, two beams (main beam and spar) are used in the length of the blade, as shown in **Figure 1**.

Length (m)	Attack degree (O)	Chord length (m)		Twist		Distance end section to hub (O)	Airfoil type (NACA)
		Root	Tip	(m)	(O)		
21	14	2	0.4	15	3.50		NACA 63 <sub>2</sub> – 415

**Table 1.** Geometric dimensions of 660 kW wind turbine blades.

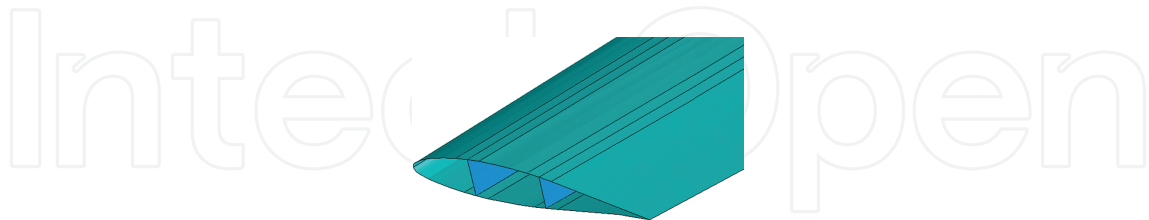


**Figure 1.** Section of two beams in the length of blade.

Section of the blade has taper as well as twist in the length of the blade in which the amount of twist in the tip of the blade as compared to the root is  $15^\circ$  (**Figure 2**). According to the physics and geometry of the blade, in order to have the layup ability of the structure, the Shell99 element for meshing is selected. To simulate the structure of the blade, it is divided into five distinct regions, including shell, three parts of the main beam, and the spar, and the special layup is used for each part. The number of extractions of optimal elements carried out for analysis of the blade is known as convergence analysis. The number of optimal element of the structure is about 33,200. Three-dimensional FEM of turbine blade is shown in **Figure 3**.

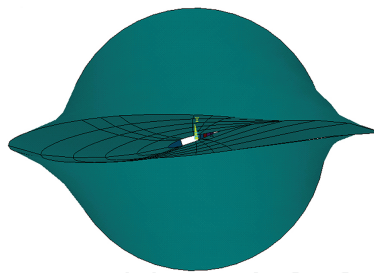


**Figure 2.** Twist of the airfoil tip of the blade in relation to its root.

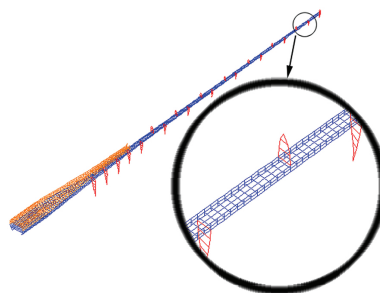


**Figure 3.** Three-dimensional FEM of the turbine blade.

### 3.2. Aerodynamic loading

The resultant of the aerodynamic forces into an airfoil section is generally shown as the lift and drag forces. By using lift and drag forces, the force  $F_Q$  that causes creation of a useful torque in the direction of rotor's rotation, and the force  $F_T$  that applies an axial force to the blades, are calculated. By integration of the moment  $\Delta Q$  and the thrust  $\Delta T$  in the length of the blade, bending moment  $M_T$  and rotation moment  $M_Q$  can be obtained. The value of the torque and thrust axial force for each section from Glauert vortex theory is determined [20–22].

$$\begin{aligned}\Delta Q &= 0.5\rho\omega^2r(C_l \sin\varphi - C_d \cos\varphi)C\Delta r \\ \Delta T &= 0.5\rho\omega^2r(C_l \cos\varphi + C_d \sin\varphi)C\Delta r\end{aligned}\quad (1)$$

$$\begin{aligned}F_Q &= L \sin\varphi - D \cos\varphi \\ F_T &= L \cos\varphi + D \sin\varphi\end{aligned}\quad (2)$$

where  $C$  is chord length,  $r$  is radius,  $\omega$  is angular speed, and  $\rho$  is air density. The  $C_l$ ,  $C_d$ ,  $L$ , and  $D$  indicate the lift and drag coefficients, and lift and drag forces, respectively. The diagram of these forces is shown in **Figure 4**. In this figure,  $W$  indicates the relative effective wind speed on the blades and the  $\varnothing$  is the angle between the relative wind speed and the axis perpendicular to the rotation axis, which consists of the attack angle ( $\alpha$ ) and the airfoil torsion ( $\theta$ ) [20–22]. Using MATLAB software, a computer code was developed which is able to calculate the values of the forces and moments in Eqs. (1) and (2), for the blade 660 kW and are shown in **Table 2**. The above forces and moments are entered at the center of each section.

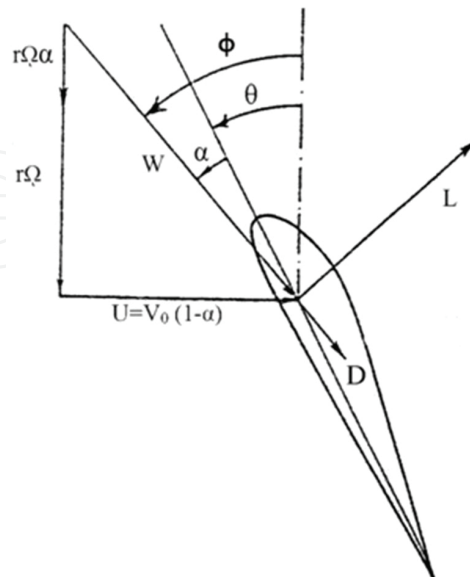


**Figure 4.** Aerodynamic forces acting on the turbine blade.

Rotation forces ( $F_Q$ )	Axial forces ( $F_T$ )	Rotation moment ( $M_Q$ )	Bending moment ( $M_T$ )
13,262 (N)	90,177 (N)	174,015 (N m)	1,291,914 (N.m)

**Table 2.** Total forces and moments on the 660 (kW) turbine blades.

### 3.3. Centrifugal force

The value of centrifugal force caused by rotor rotation with angular speed ( $\omega$ ) that in the plate rotation as tensile load, is calculated using equation  $F_{centrifugal} = mr\omega^2$ . This force depends on the angular speed of the blade and the radius rotation which is the distance from the axis of rotation to the center of mass. Angular speed of the blade is 4.45 radian per second, and hub radius of 0.8 m is considered.

## 4. Finite element analysis of the composite blade

### 4.1. Layup design

For different parts of the blade according to the applied loads, proper arrangement of the glass/epoxy laminates and foam was used [23]. The high stiffness, low density, and good fatigue performance are important for composite wind turbine blades. In **Table 3**,  $\rho$  is density,  $E_x$  and  $E_y$  are the stiffness,  $G_{xy}$  is the shear stiffness, and  $\nu_{xy}$  and  $\nu_{yx}$  are the Poisson's ratios. The thickness of each layer of composite was 0.3 mm, and the thickness of the foam was 3 mm.

$E_x$ (GPa)	$E_y$ (GPa)	$E_{xy}$ (GPa)	$\nu_{xy}$ (GPa)
76	10.3	7.17	0.28

**Table 3.** Elastic constants of glass/epoxy unidirectional ply [23].

Based on the decrease in bending moment from root to tip of the blade, there is no need to have a uniform thickness throughout the length of the beam. Therefore, it is necessary to reduce the thickness by dropping the number of composite ply in order to decline weight of the structure and to optimize the model.

Since the arrangement of the composite laminates, it should be noted that the flange beam bears the bending forces and the web section transfers the shear stress. Therefore, stacking sequences in the flange in the zero layers and layup in the web section have  $\pm 45$  angle relative to the longitudinal axis of the blade. The results of the analysis of the metal model confirm this result, and the direction of the principle stresses in the metal model indicates the layup of laminate in the composite blade [21]. Stacking sequences of the shell is  $[\pm 54_5 / C / \pm 45_5]$ , and its thickness is 6 mm. The main and the secondary beam layup are shown in **Table 4**.

Main beam	Stacking sequences in web	Thickness in web	Stacking sequences in flange	Thickness in flange (mm)
Root to 7 m	$[\pm 54_{10} / C / \pm 45_{10}]$	9	$[0]_{46}$	13.8
From 7 to 14 m	$[\pm 54_9 / C / \pm 45_9]$	8.4	$[0]_{36}$	10.8
From 14 to 21 m	$[\pm 54_8 / C / \pm 45_8]$	7.8	$[0]_{20}$	6
Spar	$[\pm 54_7 / C / \pm 45_7]$	7.2	$[0]_{20}$	6

Table 4. Layup design of beam and spar for 660 kW turbine blades.

### 4.2. Stress analysis

Stress analysis is a major topic in the wind turbine blades which is performed by software program. The stress and strain at different directions are considered in order to control the safety factor of the blade against applied loads. The most important parameter in the stress analysis of the blades is the maximum stresses and critical values. For a composite blade, the normal and shear stresses are calculated initially and then the stresses are analyzed based on the Tsai-Wu failure criterion. Moreover, stress contour must be studied in the critical layer because the possibility of failure is highest in the whole structure.

From the theoretical point of view, the stress in the area of the blade root which is under the influence of aerodynamic forces, weight force, and maximum bending moment is higher than other parts of the blade.

Figure 5(a)

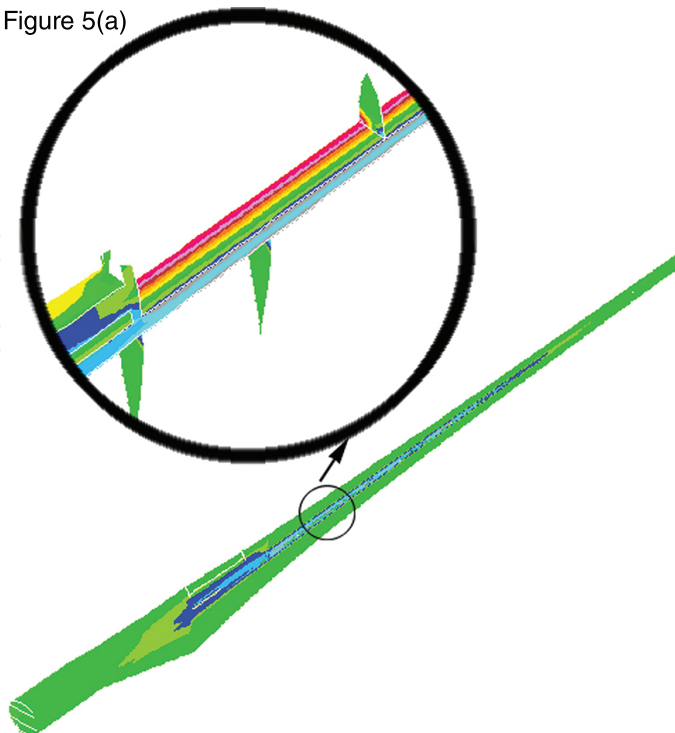
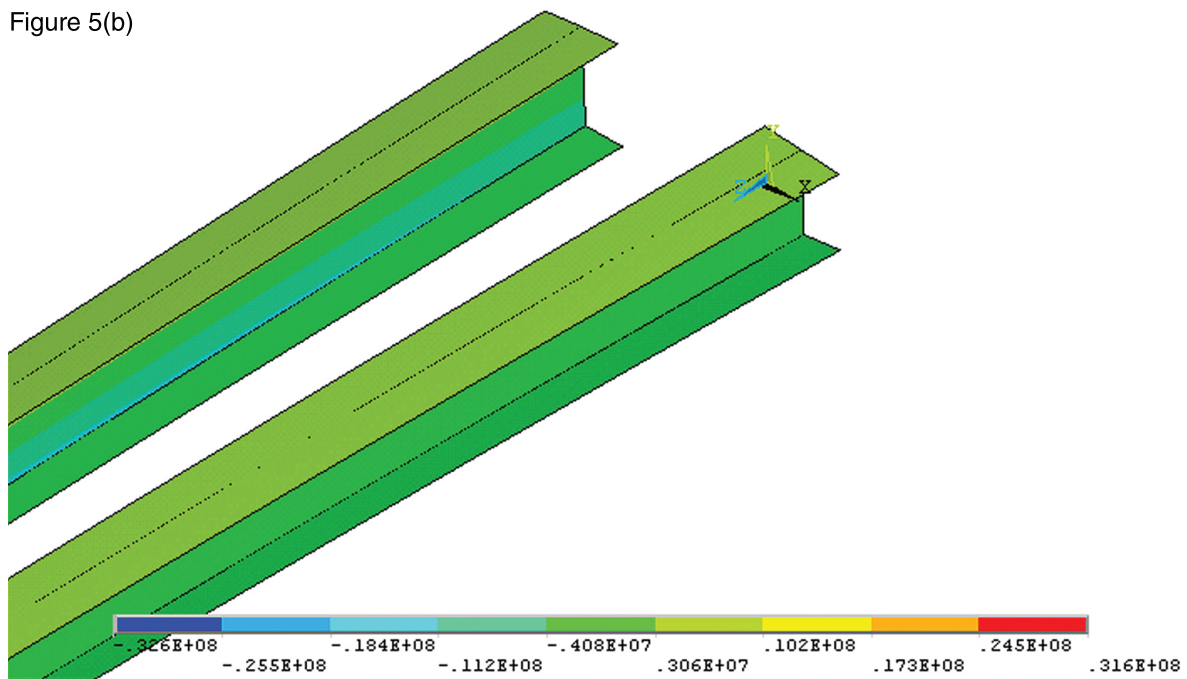
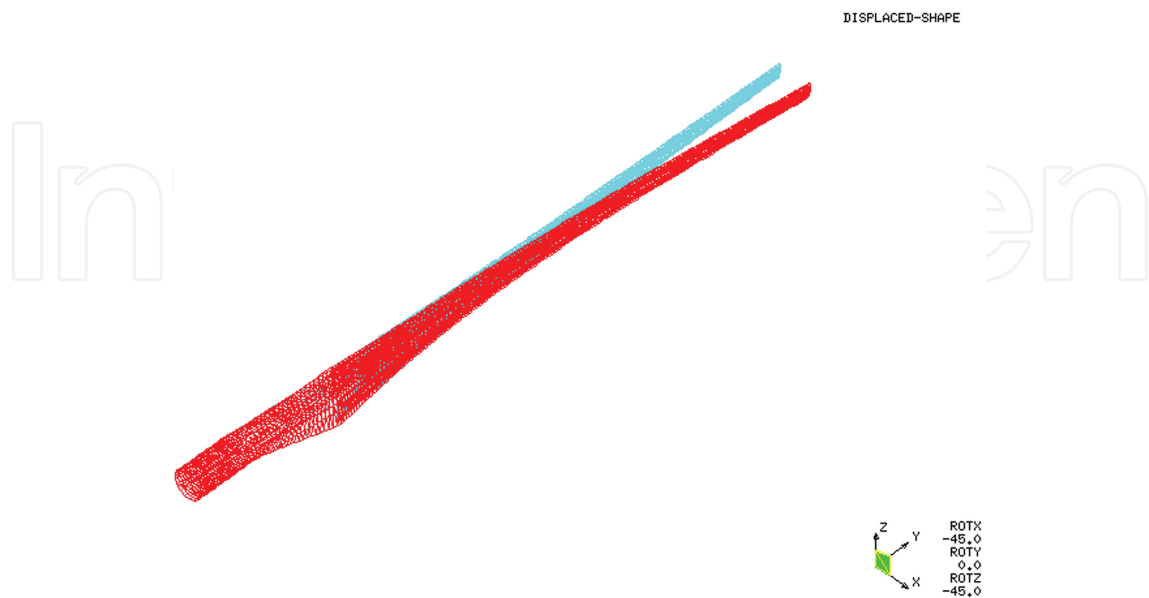


Figure 5(b)



**Figure 5.** The stress contours in the critical layer of main beam: (a) stress in fiber direction (b) stress in transverse direction.

Furthermore, according to the layer properties of the composites, it is necessary that stress contour in the critical layer in which the possibility of failure is highest in the whole structure be studied. In this study, the critical values are extracted by investigating the stress in fiber direction, perpendicular to fiber (transverse) direction, and the shear stress. The stress contours in the beam and spar critical layer with maximum failure stress number is shown in **Figure 5**.



**Figure 6.** Deflection of the 660 kW turbine blades.

In order to study the safety factor of static design, Tsai-Wu failure criterion was used. Minimum safety factor for destruction in the critical layer is obtained equal to 4. Also, during rotor performance, the maximum displacement of the blades is 1.4 m where the angle of the blade is  $3.81^\circ$  deflection at the tip [21]. This indicates a considerable improvement over similar models. The deflection of composite wind turbine blade is shown in **Figure 6**. The minimizing blade tip deflection and the sufficient distance between blade and tower in critical conditions are very important.

### 4.3. Vibration analysis

Dynamic effects in mechanism of the wind turbine due to frequency of aerodynamic loads during normal rotation are significant. In structural engineering, modal analysis uses the overall mass and stiffness of a structure to find the various periods at which it will naturally resonate. The modal analysis for structural mechanics is performed in order to obtain the natural mode shapes and frequencies of a structure. This analysis is carried out by the FEM. In order to do aeroelastic analysis and ensure the non-occurrence of flutter phenomenon, modal analysis of composite structures, natural frequencies with their mode shapes are studied. The results of modal analysis of structure using FEM up to 10 natural frequencies are expressed in **Table 5**.

Number mode	1	2	3	4	5	6	7	8	9	10
Natural frequency (Hz)	0.89	2.52	2.98	5.44	8.51	9.41	10.63	14.82	15.72	16.35

**Table 5.** Natural frequencies of the 660 kW composite wind turbine blade.

## 5. Aeroelastic analysis

One of the important topics for designing of the wind turbines blades is aeroelasticity phenomenon, because it is the major source of instability in the blades. Flutter is the coupling between bending and torsional vibration of the flexible bodies which is one of the instability factors. There are different models to analyze the flutter such as simple, spring restrained, and rigid wing that in the rigid wing model, the discrete springs would reflect the wing structural bending and torsional stiffnesses, and the reference point would represent the elastic axis [24]. To prevent the aeroelasticity instability due to the flutter in the blades, JAR-23 [2] standard is proposed. Using the JAR-23 and isolating the natural frequencies of the bending and torsional, the blade can be protected against flutter in the close of fluid velocity.

### 5.1. Numerical aeroelastic of a blade

The bending and torsion modes related to these frequencies should be identified and separated by finding the values of natural frequencies.

According to JAR-23 standard, flutter phenomenon occurs when both bending and torsion sequential modes are overlapped. Therefore, flutter safety factor of blades equals the ratio of

two consecutive bending and torsion modes of blades. Structural analysis of composite blade value and safety factor ( $n_1$ ) is calculated as follows:

$$n_1 = \frac{\omega_b}{\omega_\theta} = \frac{14.82}{10.63} = 1.39 \quad (3)$$

where  $\omega_b$  and  $\omega_\theta$  are bending and torsional frequencies, respectively. The torsional and bending modes of composite blade structure are shown in **Figures 7 and 8**. The reason for this choice is the lowest ratio between two successive bending and torsional modes. Obtained minimum safety factor is acceptable. Therefore, FEM shows that structural safety and aeroelastic stability are reliable.

```
DISPLACEMENT
STEP=1
SUB =7
FREQ=10.634
DMX =.054335
```

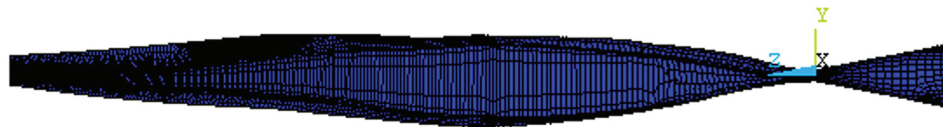


**Figure 7.** Torsion mode of the 660 kW composite wind turbine blade.

```
DISPLACEMENT
STEP=1
SUB =8
FREQ=14.806
DMX =.126475
```



**Figure 8.** Bending mode following torsion mode of the 660 (kW) composite wind turbine blade.

### 5.2. Analytical aeroelastic of a blade

In this section, the two-dimensional analytical study of aeroelastic stability for composite wind turbine blade was carried out with two degrees of freedom. Flutter analysis was often performed using simple, spring restrained, and rigid wing models such as the one shown in **Figure 9**. In the later, the discrete springs would reflect the wing structural bending and torsional stiffnesses, and the reference point would present the elastic axis [24]. The points  $P$ ,  $C$ ,  $Q$ , and  $T$  refer to the reference point, the center of mass, the aerodynamic center, and the three-quarter-cord, respectively. The dimensionless parameters  $e$  and  $a$  determine the location of the point  $C$  and  $P$  when these parameters are zero, the point lies on the mid cord, and when they are positive/negative, the points lie toward the trailing/leading edge. Also,  $b$  is a reference of semi-chord of the lifting surface.

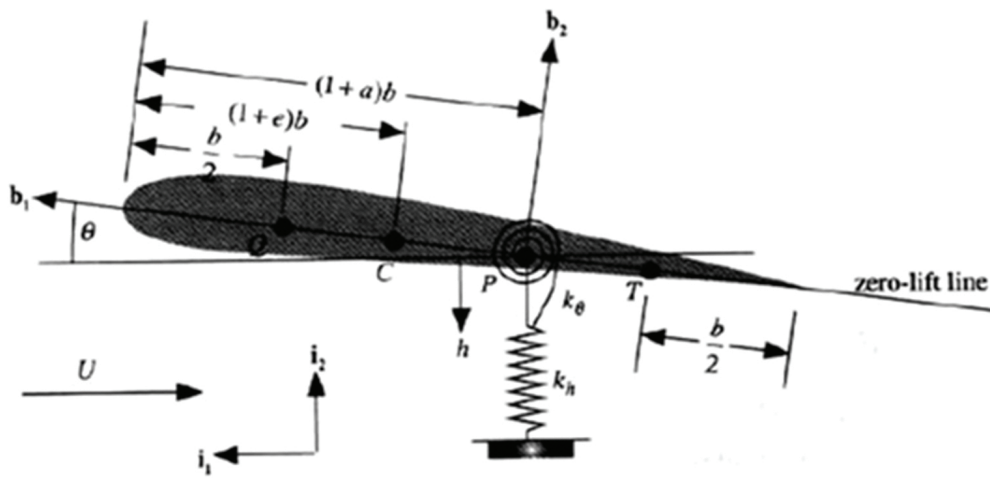


**Figure 9.** Two-dimensional aeroelastic modeling of airfoil with two-degree freedom.

The chordwise offset of the center of mass from the reference point is defined as follows:

$$x_{\theta} = e - a \tag{4}$$

The rigid plunging and pitching of the model is restrained by light, linear spring with spring constants  $k_h$  and  $k_{\theta}$ . It is convenient to formulate the equations of motion from Lagrange’s equations. To do this, one needs kinetic and potential energies as well as the generalized forces resulting from aerodynamic loading. The potential ( $P$ ) and kinetic ( $K$ ) energies are given by the following formula [24]:

$$\begin{aligned}
 P &= \frac{1}{2}k_h h^2 + \frac{1}{2}k_{\theta} \theta^2 \\
 K &= \frac{1}{2}m v_c^2 + \frac{1}{2}I_c \dot{\theta}^2
 \end{aligned}
 \tag{5}$$

where  $c$  is the mass center and  $I_c$  is the moment of inertia about  $c$ . In addition,  $m$  is mass and  $v_c$  is the velocity of mass center. The degrees of freedom  $h$  and  $\theta$  are easily derived from the work done by the aerodynamic lift  $L$ , through a virtual displacement of point  $Q$  and the aerodynamic pitching moment about  $Q$  through a virtual rotation of the modal.

Using simplicity in Lagrange's formalism for the aerodynamics equation of motion can be presented as follows [24]:

$$\begin{aligned} m(\ddot{h} + bx_\theta\ddot{\theta}) + k_h h &= -L \\ I_p\ddot{\theta} + mbx_\theta\dot{h} + k_\theta\theta &= b(0.5 + a)L \end{aligned} \quad (6)$$

where  $L$  is Lagrangian and  $I_p = I_c + mb^2x_\theta^2$ . To simplify the formula, we introduce the uncoupled, natural frequencies at zero airspeed, represented by the following:

$$\omega_h = \sqrt{\frac{k_h}{m}}, \quad \omega_\theta = \sqrt{\frac{k_\theta}{I_p}} \quad (7)$$

To introduce dimensionless variables to further simplify the problems, we consider the following four parameters:

$$r^2 = \frac{I_p}{mb^2} \quad \sigma = \frac{\omega_h}{\omega_\theta} \quad \mu = \frac{m}{\rho \pi b^2} \quad V = \frac{U}{b\omega_\theta} \quad (8)$$

where  $r$  is the dimensionless radius of gyration of the wing about the reference point  $P$  with  $r^2 > x_\theta^2$ ;  $\sigma$  is the ratio of uncoupled bending to torsional frequencies,  $\mu$  is the mass ratio parameter reflecting the relative importance of the model mass to the mass of the air affected by the model, and  $V$  is the dimensionless free stream speed of the air that is sometimes called the reduced velocity. The equations may be simplified as follows:

$$\begin{bmatrix} s^2 + \sigma^2 & s^2x_\theta + \frac{2V^2}{\mu} \\ s^2x_\theta & s^2r^2 + r^2 - \frac{2V^2}{\mu}(\frac{1}{2} + a) \end{bmatrix} \begin{Bmatrix} \bar{h} \\ \bar{\theta} \end{Bmatrix} = \begin{Bmatrix} 0 \\ 0 \end{Bmatrix} \quad (9)$$

For a nontrivial solution to exist, the determinant of the coefficient matrix must be set equal to zero. There are two complex conjugate pairs of roots, say  $s_{1,2} = \frac{(\Gamma_{1,2} \pm i\Omega_{1,2})}{\omega_\theta}$ . For a given configuration and altitude, one must look at the behavior of the complex roots as functions of  $V$  and find smallest value of  $V$  to give divergent oscillations, whose value is  $V_F = \frac{U_F}{b\omega_\theta}$ , where  $U_F$  is the flutter speed.

For looking at flutter, we consider a specific section of a composite blade of wind turbines, defined by  $a = 0.2$ ,  $e = 0.1$ ,  $\mu = 20$ ,  $r^2 = 0.24$ , and  $\sigma$  is obtained from numerical solution. Plots of the imaginary part of the roots versus  $V$  are shown in **Figure 10**. The modal frequency of critical torsional and bending modes is shown in **Figure 10**. In **Figure 10**, when  $V = 0$ , one expects the two-dimensionless frequencies to be close unity and  $\sigma$  represents pitching and plunging oscillations, respectively. Even at  $V = 0$ , these modes are lightly coupled because of the nonzero off-diagonal term  $x_{(\theta)}$  in the mass matrix. As  $V$  increases, the frequencies start to approach one another, and their respective mode shapes exhibit increasing coupling between plunge and pitch. Flutter occurs when the two modal frequencies come close, at which point the roots become complex conjugate pairs. Under this condition, both modes are highly coupled pitch-plunge oscillations. For this composite blade of wind turbine, the flutter speed is  $V_F = U_F/b\omega_\theta = 3.306$ , and the flutter frequency is  $\Omega_F/\omega_\theta = 0.802$ .

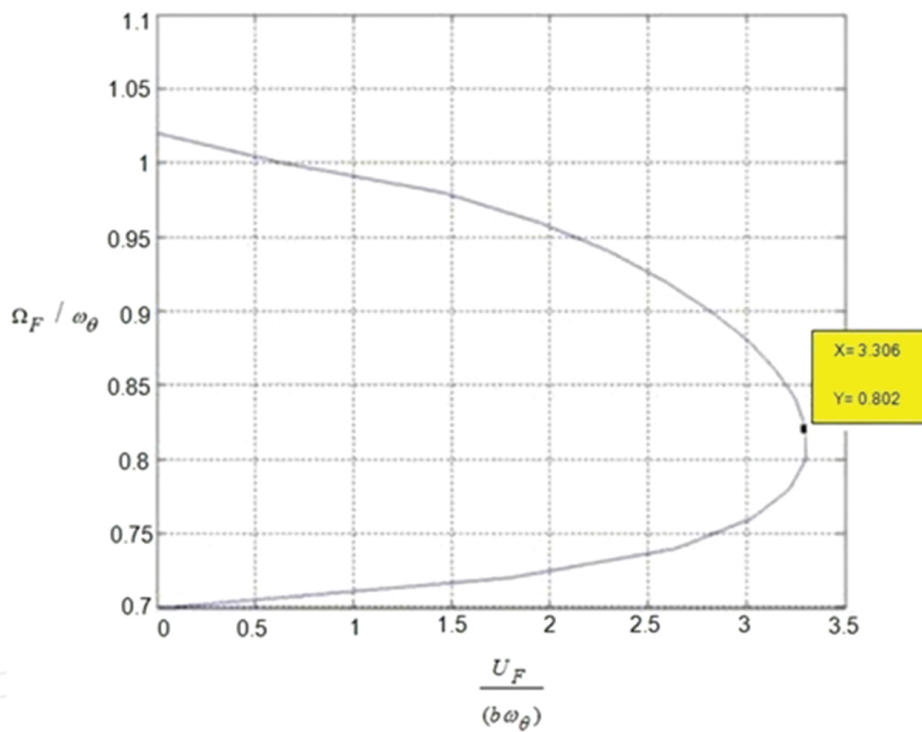


**Figure 10.** Modal frequency via  $V$  for critical torsional and bending modes.

According to the values of modal analysis and natural frequency of the torsion mode, the flutter speed is determined as follow:

$$U_F = 3.31 \times b\omega_\theta = 35 \text{ m/s} \quad (10)$$

In Eq. (10),  $b = 1$  is the half of chord length and  $\omega_\theta = 10.63$ . The relative real speed of the turbine performance is calculated as follows:

$$V = \sqrt{V_{rel}^2 + V_a^2} = 25.3 \text{ m/s} \quad (11)$$

Given the flutter speed and the performance speed of the wind turbine, safety factor can be calculated as follows:

$$n_2 = \frac{U_F}{V} = 1.38 \quad (12)$$

Obtained safety factor is acceptable and shows the safety and aeroelastic stability of the structure in the performance and design of turbine blades.

## 6. Fatigue

One of the other basic topics for designing of the wind turbines specifically for the blades is fatigue considerations. The lifetime of a wind turbine blade is estimated about 20–30 years. This long lifetime bring some design constraints for the wind turbine blades which fall into the fatigue categories.

### 6.1. Accumulated fatigue damage modeling

One of the important issues in composites is fatigue. Shokrieh and Lessard [25] presented “generalized material property degradation technique,” which is used for studying the fatigue. In this research, their technique is modified to simulate the laminated composite behavior under uni-axial fatigue loading. It means that by this model which is called “accumulated fatigue damage model”, damage status at every level and the number of cycles from start of loading to sudden failure of the component are estimated and subsequently final fatigue life is predicted. Three different sections of this model are including stress analysis, damage estimation, and material properties degradation. Classical lamination plate theory (CLPT) is proper because the effect of edge will not occur due to placing the selected critical zone in a confined region. The flowchart of the accumulated fatigue damage is shown in **Figure 11**.

As depicted in **Figure 11**, in the first step, a proper model for stress analysis must be developed, which have defined different parameters including material properties, maximum and minimum fatigue load, maximum number of cycles, incremental number of cycles. In the second step, failure analysis is done so that if a sudden mode of failure exists, the material properties of the failed plies are changed according to the appropriate sudden material property degradation rules. Then, the stress and failure analyses are carried out again according to the new stiffness matrix of the FEM. In this step, if there is no sudden mode of failure, an incremental number of cycles is applied. The computer program stops if the number of cycles is greater than a preset total number of cycles. Otherwise, the gradual material property degradation rules are applied for changing the stiffness of all plies (of all elements).

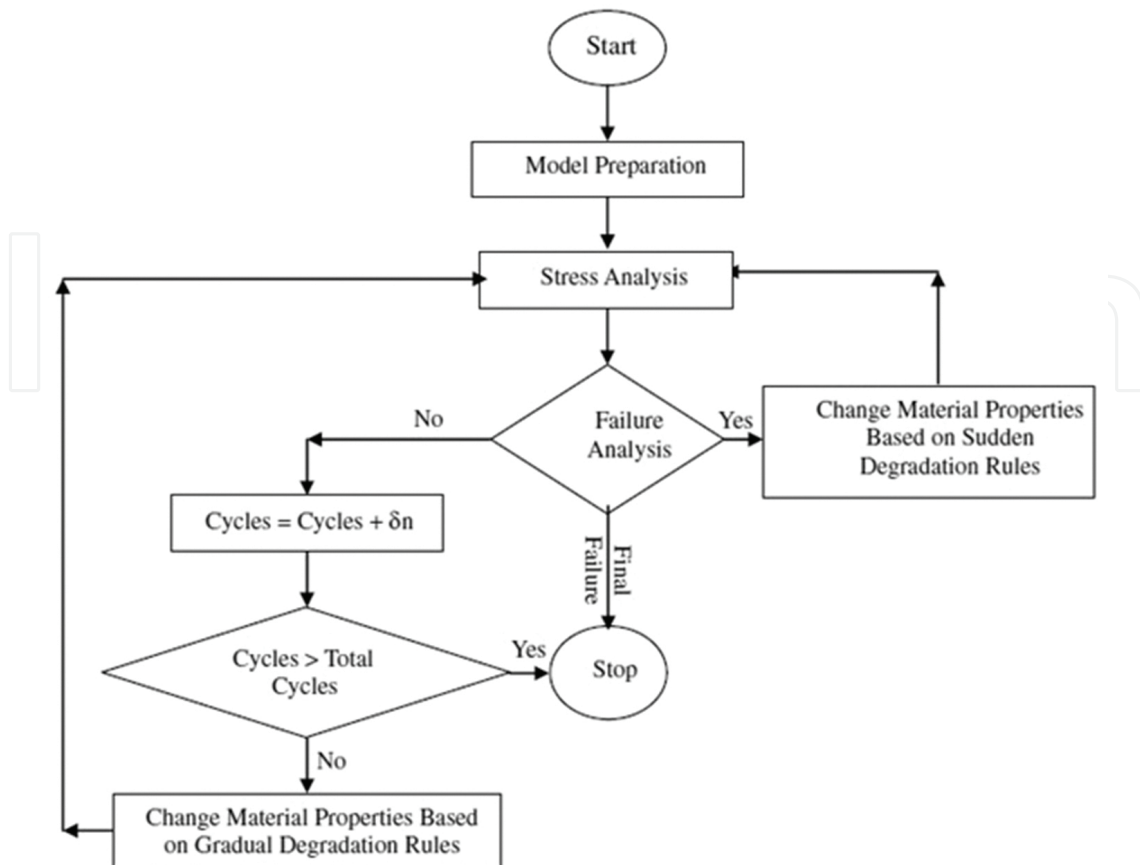


Figure 11. Flowchart of accumulated fatigue damage modeling.

The depicted loop is repeated until a failure occurs or the maximum number of cycles, which has been defined by the user, is reached. In this section, the stiffness degradation method is applied because one of the aims is decreasing the run-time of the model. In this method, remaining stiffness of an U-D ply under desired uni-axial state of stress and desired stress ratio can be calculated using the following equation which is a modified and improved form of Ye's model [26]:

$$E(n, \sigma, \kappa) = \left( 1 - \frac{\tilde{D}}{f(\sigma, \sigma_{ult})} \right) E_0 \quad (13)$$

where  $E_0$ ,  $E(n, \sigma, \kappa)$ , and  $\tilde{D}$  are initial stiffness before start of fatigue loading, residual stiffness (as a function of number of cycles, applied stress, and stress ratio) and normalized damage parameter, respectively. It is necessary to mention that the role of stress is included in the amount of damage using  $f(\sigma, \sigma_{ult})$  because amount of  $\tilde{D}$  does not depend on the applied stress level. A complete form of  $f(\sigma, \sigma_{ult})$  was developed [25] based on available experimental data for carbon/epoxy (commercially called AS4/3501-6). A developed method is utilized for

damage estimation, which is called the normalized number of cycles, and it calculates  $D'$ , which describes a relation between  $\tilde{D}$  and  $\tilde{N}$ . Available experimental data show that normalized damage increases linearly from start of loading till  $\tilde{N} = 0.67$  and after that the rate of damage increases non-linearly until final failure ( $\tilde{N} = 1$ ). Therefore, the relation between  $\tilde{D}$  and  $\tilde{N}$  can be divided into two phases. All the linear and non-linear relations between  $\tilde{D}$  and  $\tilde{N}$  are presented for both phases [27] that in those relations,  $\tilde{N}$  is obtained using the following equation:

$$\tilde{N} = \frac{\log(n) - \log(0.25)}{\log(N_f) - \log(0.25)} \quad (14)$$

where,  $n$  and  $N_f$  describe number of applied cycles and cycles to failure, respectively.  $N_f$  must be calculated using following relation [25]:

$$\frac{\ln(a/f)}{\ln[(1-q)(C+q)]} = A + B \log N_f \quad (15)$$

where

$$q = \sigma_m / \sigma_t \quad a = \sigma_a / \sigma_t \quad C = \sigma_c / \sigma_t \quad \sigma_m = \frac{(\sigma_{\max} + \sigma_{\min})}{2} \quad \sigma_a = \frac{(\sigma_{\max} - \sigma_{\min})}{2} \quad (16)$$

It is shown that in shear loading, the aforementioned equation can be modified to the following form [25]:

$$u = \log \left( \frac{\ln(a/f)}{\ln[(1-q)(C+q)]} \right) = A + B \log N_f \quad (17)$$

where  $u$  and  $f$  are curve fitting parameters, which have been obtained for AS4/3501 material [25].

## 6.2. Evaluation of accumulated fatigue damage model

The results have been calculated for a 0-degree unidirectional ply (U-D) of carbon/epoxy under tensile longitudinal fatigue loading, a 90-degree U-D ply of carbon/epoxy under tensile transverse fatigue loading and a cross-ply of carbon/ epoxy which are shown in **Figures 12–14**, respectively, and compared with the experimental results [25, 28, 29]. The results demonstrate that the presented model has appropriate performance.

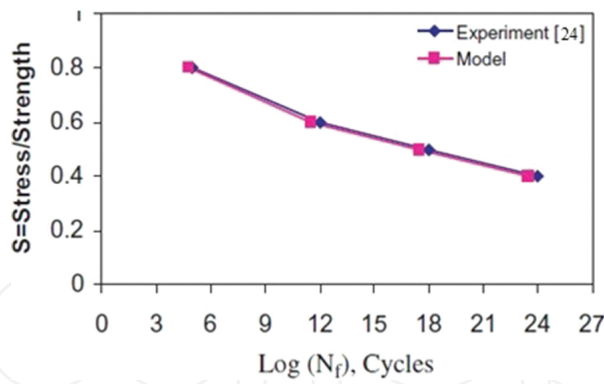


Figure 12. Experimental data and results of computer code for 0-degree ply.

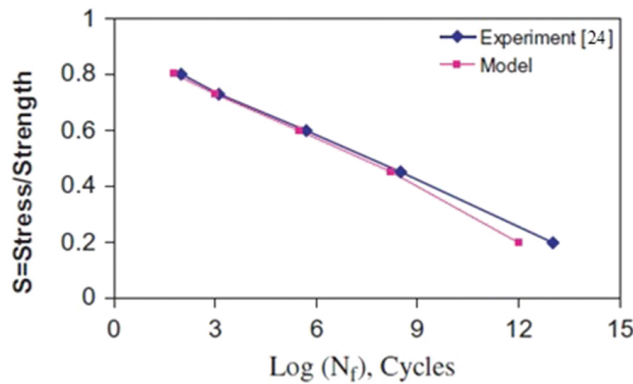


Figure 13. Experimental data and results of computer code for 90-degree ply.

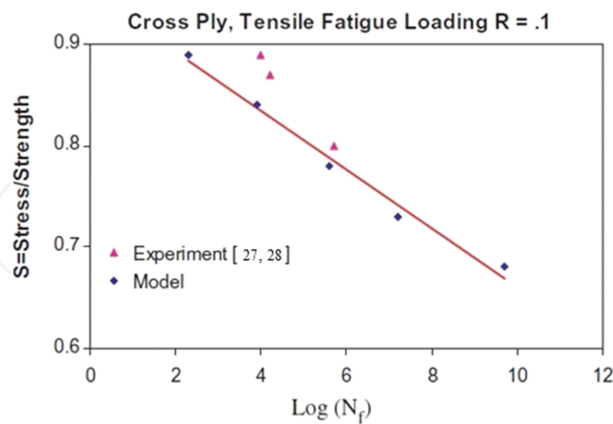


Figure 14. Experimental data and results of computer code for cross ply.

All equations and relations have been developed based on available experimental data for carbon/epoxy composites. Since normalized life curves for glass/epoxy were not available, a generic behavior was estimated based on the pattern of decreasing mechanical properties and strengths of carbon/epoxy. The only available criteria for the evaluation of aforementioned

generic fatigue behavior process are the mentioned criteria in Montana State University/ Department of Energy (MSU/DOE) fatigue database [30] for wind turbine blade application. In MSU/DOE, the behavior of involved composite materials in blade structures is defined by the following equation:

$$\sigma/\sigma_0 = 1 - b \log(N) \tag{18}$$

where  $\sigma$ ,  $\sigma_0$ , and  $b$  are maximum applied stress, corresponding static strength in the same direction of applied stress and a parameter which varies for the different materials, respectively. In MSU/DOE, two magnitudes of “ $b$ ” were presented which describe two boundaries of all curves. The upper and lower bounds refer to good and poor materials, respectively, which behave perfectly and weakly against fatigue. The values of “ $b$ ” for different fatigue loading situations [30] are presented in **Table 6**.

Type of data	Extremes of normalized S-N fatigue data for fiberglass laminates		
Tensile fatigue data ( $R = \sigma_{\min} / \sigma_{\max} = 0.1$ )	Good materials ( $b = 0.1$ )	Poor materials ( $b = 0.14$ )	Normalization <i>UTS</i>
Compressive fatigue data ( $R = 10$ )	Good materials ( $b = 0.07$ )	Poor materials ( $b = 0.11$ )	Normalization <i>UCS</i>
Reversal fatigue data ( $R = -1$ )	Good materials ( $b = 0.12$ )	Poor materials ( $b = 0.18$ )	Normalization <i>UTS</i>

<sup>a</sup>Ultimate tensile strength.

<sup>b</sup>Ultimate compressive strength.

**Table 6.** Values of “ $b$ ” for two bounds of good and poor materials (S-N data).

The results of tensile mode based on the generic method with good [30] and poor materials are indicated in **Figure 15**. It is found that the results are logical and the generic behavior is proper because the pre-preg materials have high quality and same volume of resin at all points containing non-woven fabrics.

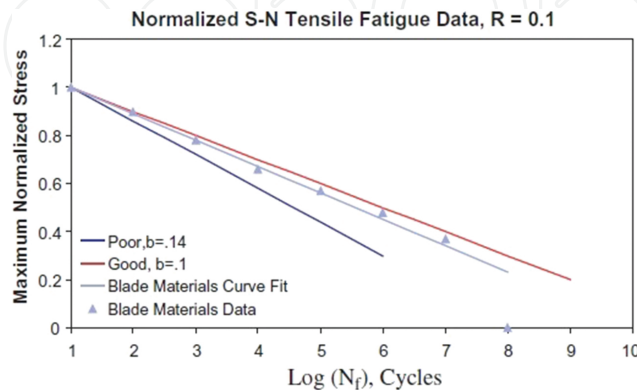


**Figure 15.** Results of computer code based on used generic method in comparison with good and poor material data from MSU/DOE database.

One of the most important advantages of using accumulated fatigue damage modeling is in its independence of layup configuration. Thus, it can be used for any configuration of fabrics, knowing behavior of involved U-D plies (full characterization of each configuration is not required).

### 6.3. Wind resource characterization

One of the most important issues for fatigue analysis is identification of governing wind patterns on the wind farm vicinity. The wind speed is never steady at any site because different parameters influence on it such as the weather system, the local land, and the height above the ground surface. Therefore, average wind speed should be obtained over a long term, for example, 10 or more years to raise the confidence in wind speed distribution. However, long-term measurements are expensive, and most projects cannot wait that long.

The “measure, correlate, and predict (MCP)” technique is used instead of long-term measurements so that short term, for example, one year is considered and data are compared with available long-term data of a near site. By this technique, the long-term annual wind speed at the site under consideration is obtained.

The Weibull function of Manjil (a city in the north of Iran), which can describe the wind speed variations over the period, was derived using metrological data in the following form [31]:

$$h(v) = \left( \frac{1.425}{9.3206} \right) \left( \frac{v}{9.3206} \right)^{(0.425)} e^{-\left( \frac{v}{9.3206} \right)^{1.425}} \quad (19)$$

where  $v$  and  $h(v)$  are wind speed and the corresponding probability of occurrence, respectively. This distribution is shown in **Figure 16**.

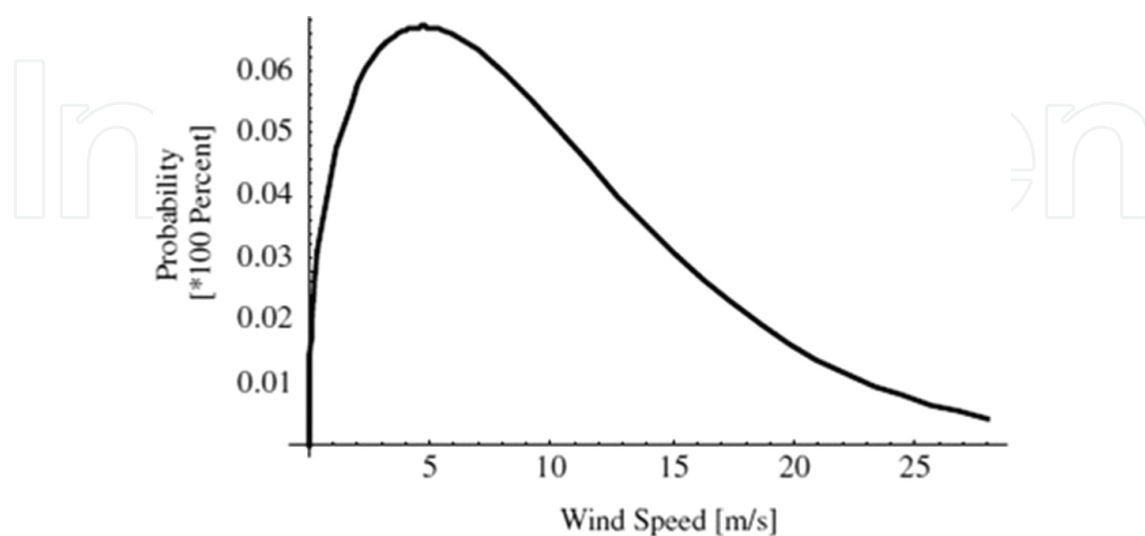


**Figure 16.** Weibull distribution function of Manjil.

#### 6.4. Investigation on fatigue of the blade

There are different sources which produce cyclic loads on a wind turbine blade. Some of them are the variation of wind speed, annual gust, rotation of rotor, and variation of weight vector direction toward the local position of the blade [31]. The variation of wind speed and annual gust produces cyclic loads by changing the total amount of the load. Also, fluctuating load is produced by the rotation of rotor. In addition, the effect of wind shear, which arises from change of wind speed by change in height, causes cyclic loading. In the usual calculation, wind speed is measured at the hub center of rotor. So, the effect of wind shear is neglected because it has a negligible effect on the fatigue damage [18]. Therefore, this effect is not considered further in the design process. It has been proven that the wind shear effect acts in-phase with the weight vector.

The estimated lifetime of the blade by the computer code, which was executed 50 times, is shown in **Figure 17**. The results show that the maximum and minimum lifetimes are 24 and 18.66 years, respectively, and the average is 21.33 years. Further, 1.59 years are the standard deviation of the obtained results.

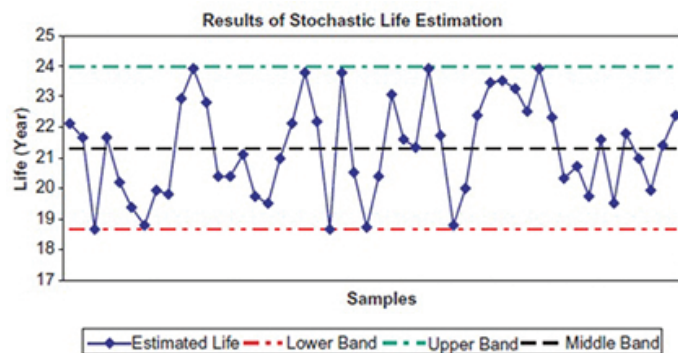


Figure 17. Predicted lifetime of the blade by computer code and for 50 runs.

## 7. Conclusion

In this chapter, the aerodynamic loading, design, static analysis, dynamic analysis, aeroelastic stability, and fatigue of composite wind turbine blades were considered. Aerodynamic loading with weight and the centrifugal loading to the blade was applied. Safety factor for failure in the composite model using Tsai-Wu failure criterion for the critical layer was obtained. In the FEM, using modal analysis and extracting natural frequencies and aeroelastic stability of structure, the safety factor was calculated and was equal to 1.39. In analytical method, the changes in natural frequencies of the system due to free stream speed were studied and flutter speed related to the coupling of bending and torsion was obtained. According to speed performance of turbine, safety factor of aeroelastic stability equivalent to 1.38 was calculated. Obtained safety factor was acceptable in all stages and indicates the stability and safety of composite blades structure in static, dynamic, and aeroelastic design. The accumulated fatigue

damage model was presented and applied based on CLPT. Furthermore, fatigue phenomenon was studied in the selected critical zone using accumulated fatigue damage modeling. The results of fatigue demonstrated that 24 and 18.66 years are the lower and upper limits, respectively. These results showed that the presented accumulated fatigue damage model was able to simulate the fatigue damage progress in a wind turbine composite blade. Considering the conservative nature of the employed technique, the investigated blade had 18.66 years in the worse situation and 24 years in the best situation.

## Acknowledgements

The authors are grateful to the University of Kashan for supporting this work by Grant No. 463853/03.

## Author details

Ahmad Reza Ghasemi\* and Masood Mohandes

\*Address all correspondence to: Ghasemi@kashanu.ac.ir

Department of Solid Mechanics, Faculty of Mechanical Engineering, University of Kashan, Kashan, Iran

## References

- [1] Jureczko M, Pawlak M, Mezyk A. Optimisation of wind turbine blades. *Journal of Materials Processing Technology*. 2005; 167, 463–471. doi:10.1016/j.jmatprotec.2005.06.055
- [2] Guo S. Aeroelastic optimization of an aerobatic aircraft wing structure. *Aerospace Science and Technology*. 2007; 11, 396–404. doi:10.1016/j.ast.2007.01.003
- [3] Veers PS, Ashwill TD, Sutherland HJ, Laird DL, Lobitz DW. Trends in the design, manufacture and evaluation of wind turbine blade. *Advances in Wind Energy*. 2003; 6, 254–259. doi:10.1002/we.90
- [4] Baumgart, A. A mathematical model for wind turbine blades. *Journal of Sound and Vibration*. 2002; 251, 1–12. doi:10.1006/jsvi.2001.3806
- [5] Larsen JW, Nielsen SR. Nonlinear parametric instability of wind turbine wings. *Journal of Sound and Vibration*. 2007; 299, 64–82. doi:10.1006/jsvi.2001.3806

- [6] Petrini F, Li H, Bontempi F. Basis of design and numerical modeling of offshore wind turbines. *Structural Engineering and Mechanics*. 2010; 36, 599–624. doi:10.12989/sem.2010.36.5.599
- [7] Lee JW, Kim JK, Han JH, Shin HK. Active load control for wind turbine blades using trailing edge flap. *Wind and Structures*. 2013; 16, 263–278. doi:10.12989/was.2013.16.3.263
- [8] Tenguria N, Mittal ND, Ahmed S. Structural analysis of horizontal axis wind turbine blade. *Wind and Structures*. 2013; 16, 241–248. doi:10.12989/was.2013.16.3.241
- [9] Fung YC. *An introduction to the theory of aeroelasticity*. Dover Publications, INC, Mineola, New York; 1969.
- [10] Joint aviation requirements, (JAR-23), Normal, Utility, Aerobatic and Commuter Category Aeroplanes, Joint Aviation Authorities, Hoofddorp, The Netherlands. March 1994.
- [11] Shokrieh MM, Taheri-berooz F. Wing instability of a full composite aircraft. *Composite Structures*. 2001; 54, 335–340. doi:10.1016/S0263-8223(01)00107-6
- [12] Baxevanou CA, Chaviaropoulos PK, Voutsinas SG, Vlachos NS. Evaluation study of a Navier–Stokes CFD aeroelastic model of wind turbine airfoils in classical flutter. *Journal of Wind Engineering and Industrial Aerodynamics*. 2008; 96, 1425–1443. doi:10.1016/j.jweia.2008.03.009
- [13] Fazelzadeh SA, Mazidi A, Kalantari H. Bending-torsional flutter of wings with an attached mass subjected to a follower force. *Journal of Sound and Vibration*. 2009; 323, 148–162. doi:10.1016/j.jsv.2009.01.002
- [14] Lee JW, Lee JS, Han JH, Shin HK. Aeroelastic analysis of wind turbine blades based on modified strip theory. *J. Wind Eng. Ind. Aerod.* 2012; 110, 62–69. doi:10.1016/j.jweia.2012.07.007
- [15] Sutherland HJ. *On the fatigue analysis of wind turbines*. Sandia National Laboratories, Albuquerque, New Mexico; 1999.
- [16] Mandel JF, Samborsky DD, Cairns DS. *Fatigue of composite materials and substructures for wind turbine blades*. Sandia National Laboratories, Albuquerque, New Mexico; 2002.
- [17] Shokrieh MM, Rafiee R. Lifetime prediction of HAWT composite blade. In: 8th International Conference of Mechanical Engineering (ISME), Iran; 2004. p. 240.
- [18] Noda M, Flay RGJ. A simulation model for wind turbine blade fatigue loads. *Journal of Wind Engineering and Industrial Aerodynamics*. 1999; 83, 527–40. doi:10.1016/S0167-6105(99)00099-9

- [19] Germanischer Lloyd Rules and Guidelines Industrial Services, Part IV, Guideline for the Certification of Wind Turbines, Chapter 4, Load Assumptions, Hamburg, Germany, Edition 2010.
- [20] Eggleston DM, Stoddard FS. Wind turbine engineering design. Springer, Van Nostrand Reinhold Co. Inc., New York, USA; 1987.
- [21] Ghasemi AR, Jahanshir A, Tarighat MH. Numerical and analytical study of aeroelastic characteristics of wind turbine composite blades. *Wind and Structures*. 2014; 18, 103–116. doi:10.12989/was.2014.18.2.103
- [22] Ghasemi AR, Tarighat MH. Aeroelastic analysis of composite wind turbines blades. *Journal of Mechanical Engineering University of Tabriz*. 2015; 44, 31–39.
- [23] Tsai SW, Massard TN. Composites design (4th Ed.). Think Composites, Dayton, OH; 1984.
- [24] Hodges DH, Pierce GA. Introduction to structural dynamics and aeroelasticity. Cambridge University Press, New York, USA; 2002.
- [25] Shokrieh M, Lessard LB. Progressive fatigue damage modeling of composite materials, Part I: Modeling. *Journal of Composite Materials*. 2000; 34, 1056–80. doi: 10.1177/002199830003401301
- [26] Ye L. On fatigue damage accumulation and material degradation in composite materials. *Composite Science and Technology*. 1989; 36, 339–50. doi: 10.1016/0266-3538(89)90046-8
- [27] Shokrieh MM, Zakeri M. Evaluation of fatigue life of composite materials using progressive damage modeling and stiffness reduction. In: Proceedings of the 11th Annual Conference of Mechanical Engineering, Iran; 2003. p. 1256–1263.
- [28] Charewics A, Daneil IM. Damage mechanics and accumulation in graphite/epoxy laminates. In: Hahn HT, editor. *Composite Materials: Fatigue and Fracture*. 1986; 247–288. doi:10.1520/STP19991S
- [29] Lee JW, Daniel IM, Yaniv G. Fatigue life prediction of cross-ply composite laminated. In: Lagace PA, editor. *Composite Materials: Fatigue and Fracture*, ASTM International. 1989; 19–28. doi:10.1520/STP10406S
- [30] DOE/MSU. Composite materials fatigue database. Sandia National Laboratories, Albuquerque, New Mexico; 2003.
- [31] Shokrieh MM, Rafiee R. Lifetime prediction of HAWT composite blade. In: 8th International Conference of Mechanical Engineering (ISME), Iran; 2004. p. 240.